

Imaging Arrays for the Millimeter- and Submillimeter-Wave Region

K. Uehara, K. Miyashita, K. Natsume, K. Hatakeyama, and K. Mizuno

Research Institute of Electrical Communication, Tohoku University
2-1-1 Katahira, Aoba-ku, Sendai, 980 Japan

Abstract—We have been developing several kinds of lens-coupled antenna imaging arrays for operation at millimeter- and submillimeter-wave frequencies. The comparison of dipoles, Yagi-Uda's, trap-loaded antennas, and microstrip patches will be discussed from the viewpoint of the matching with detectors and optics. The radiation patterns and input impedance of each antenna have been calculated and measured at the model experiment. The arrays have been successfully applied to plasma diagnostics at the Tsukuba GAMMA 10 plasma machine.

I. INTRODUCTION

Millimeter and submillimeter wavelength imaging has recently become increasingly important in plasma diagnostics, remote sensing, and environmental measurements. Accordingly the high-performance multi-element quasi-optical imaging systems have been developing. Those systems require sensitive antennas and detectors, and high resolution optical systems. Planar antenna arrays with integrated detectors have led to improved sensitivity and scanning speed. We have been currently investigating several kinds of printed antennas [1,2,3], which are integrated with detectors and are combined with a low-loss dielectric substrate lens [4], which structure can eliminate RF feed cable-losses or substrate modes and can also offer mechanical stability and facility for cooling. On the other hand, those antennas require careful matching to the detectors and optics. In this paper, we will discuss the comparison of the lens-coupled printed antennas: dipoles, Yagi-Uda's, trap-loaded antennas and microstrip patches, all of which are integrated with beam-lead schottky diodes. Also the measurement of plasma density profile with an imaging array at the Tsukuba GAMMA 10 plasma machine will be shown as a practical application.

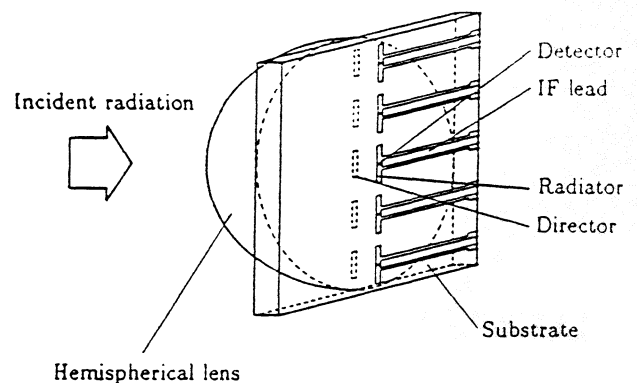
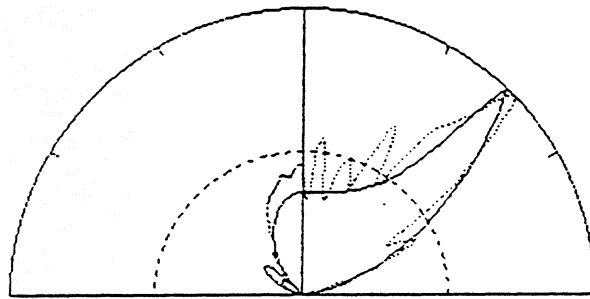


Fig. 1. Yagi-Uda antenna imaging array.

II. YAGI-UAD ANTENNA IMAGING ARRAYS

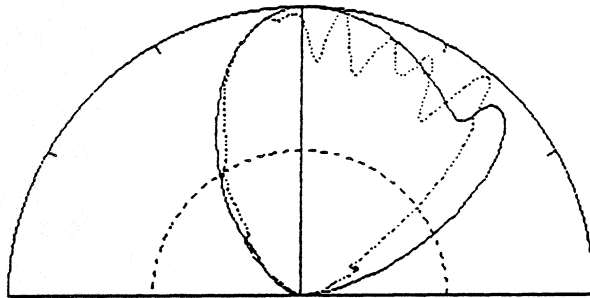
The fundamental array consists of half-wave dipoles integrated with diodes on a dielectric-air interface [1]. The input impedance of the dipole is generally much larger than that of diodes or SIS junctions, which causes large mismatch loss, because of difficulty to fabricate small-size matching circuits on the each array element. In addition, the dipole radiation pattern shows big sidelobes and large central dip in the H-plane (Fig. 2 (a)). To improve these disadvantages, we have proposed and fabricated Yagi-Uda antenna configuration [3] shown in Fig. 1. The radiator elements are photolithographically fabricated half-wave dipoles on a substrate of glass/PTFE ($\epsilon_r=2.17$), and the SBD's are integrated at the feed point of each radiator. The director elements are on the other side of the substrate to which a hyperhemispherical lens of 60mm diameter made of TPX ($\epsilon_r=2.13$) is attached. The spacing between the radiator and the director can be controlled by choosing the substrate with proper thickness. For optimization of the antenna, the element dimensions

are determined by two conditions: one is impedance matching with the detectors, and the other is beam pattern matching with the optics. The radiation pattern can be adjusted by changing the director length and the element spacing.



E-plane H-plane

(a) Dipole



E-plane H-plane

(b) Yagi-Uda

Fig. 2. The calculated and measured radiation patterns of an antenna on a dielectric hemisphere ($\epsilon_r=2.13$) of 100mm diameter. (a) Dipole, (b) Yagi-Uda ($2l_1=0.5\lambda_e$, $2l_2=0.462\lambda_d$, $d=0.093\lambda_d$). The scale is linear in power; —theory, - -experiment at 50GHz.

Fig. 2 shows optimized Yagi-Uda patterns, comparing with the dipole's. The radiator length $2l_1$ is $0.5\lambda_e$, the director length $2l_2$ is $0.462\lambda_d$, and the spacing d is $0.093\lambda_d$. λ_e and λ_d are the effective wavelength at the air-dielectric interface and the wavelength in the dielectric, respectively, being defined by

$$\lambda_e = \frac{\lambda_0}{\sqrt{(1 + \epsilon_r)/2}}, \quad (1)$$

$$\lambda_d = \frac{\lambda_0}{\sqrt{\epsilon_r}}. \quad (2)$$

The improved pattern is almost symmetrical and the directivity G_d becomes 5.5dB. The directivity is defined by

$$G_d = \frac{|D(0, 0)|^2}{\frac{1}{4\pi} \int |D(\theta, \phi)|^2 d\Omega}, \quad (3)$$

where $D(\theta, \phi)$ is the directivity function. Because the diameter of the hyperhemispherical lens is electrically enough large and the surface-wave mode can be neglected, we have applied the moment method to the dielectric half spaces to calculate current distributions on the radiator and the director. The theoretical patterns have been calculated from these current distributions. The experimental patterns were measured in a shield room at 50GHz band with a TPX hemispherical lens of 100mm diameter, being fed by the horn located at the focal point of the lens. The results agree well with the theory although many ripples are obtained in the H-planes. These ripples will be due to the effects of the radiation from the orthogonal low-frequency leads.

Also the input impedance can be tuned over a broad range by adjusting the element dimensions (Fig. 3). This method allows improved matching to low impedance detectors.

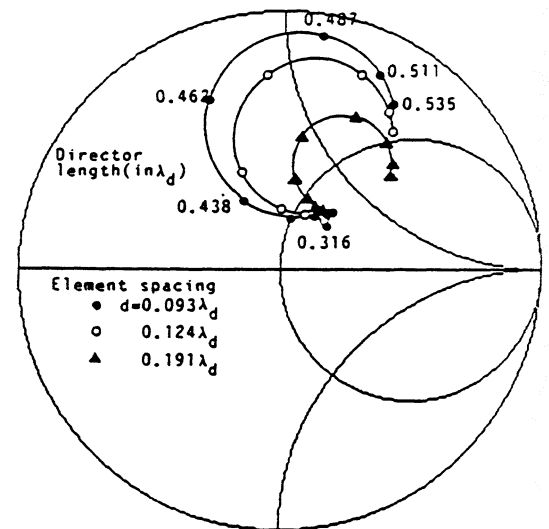


Fig. 3. The calculated input impedance of a Yagi-Uda antenna on a dielectric hemisphere ($\epsilon_r=2.13$).

Consequently good matching conditions are available without complex matching circuits. As detectors, we are using the beam-lead Schottky diode (Sanyo Electric Co. Ltd., SBL-221) with typical R_s of 5Ω , $C_j(0)$ of 0.02pF and C_p of 0.05pF , whose cutoff frequency runs into 400GHz . With an RF equivalent circuit, we have calculated the 50GHz small signal impedance of $3-j30\Omega$ at the condition of $50\mu\text{A}$ bias current. The SBD's are useful for imaging applications because they can be applicable for both video detectors and heterodyne mixers at room temperature. Fig. 4 shows calculated directivity and mismatch loss versus the director length. Considering both the impedance mismatch and directivity, we can estimate total efficiency of the individual receptor. Fig. 5 shows calculated and measured total sensitivity of the receptor. For the optimized Yagi-Uda, the receiving power from an incident plane wave is theoretically 8dB improved in comparison with the dipole, and experimentally the 6dB increased power has been measured. In the collinear Yagi-Uda array, crosstalk levels of less than 30dB down between adjacent antennas have been measured when the element interval is $0.7\lambda_d$ in 5GHz model experiments.

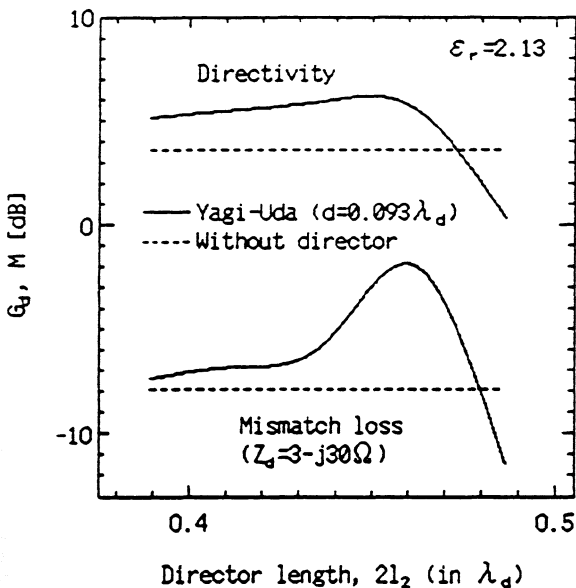


Fig. 4. The calculated directivity and mismatch loss of a Yagi-Uda antenna ($2l_1=0.5\lambda_e$, $d=0.093\lambda_d$) versus director length $2l_2$. The diode impedance is $3-j30\Omega$.

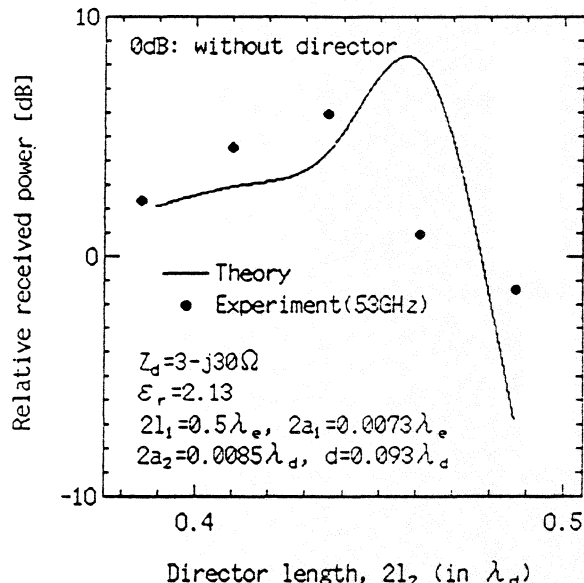


Fig. 5. Total sensitivity of a Yagi-Uda receptor versus director length $2l_2$. The 0dB line shows the sensitivity of the dipole; —theory, • experiment at 53GHz .

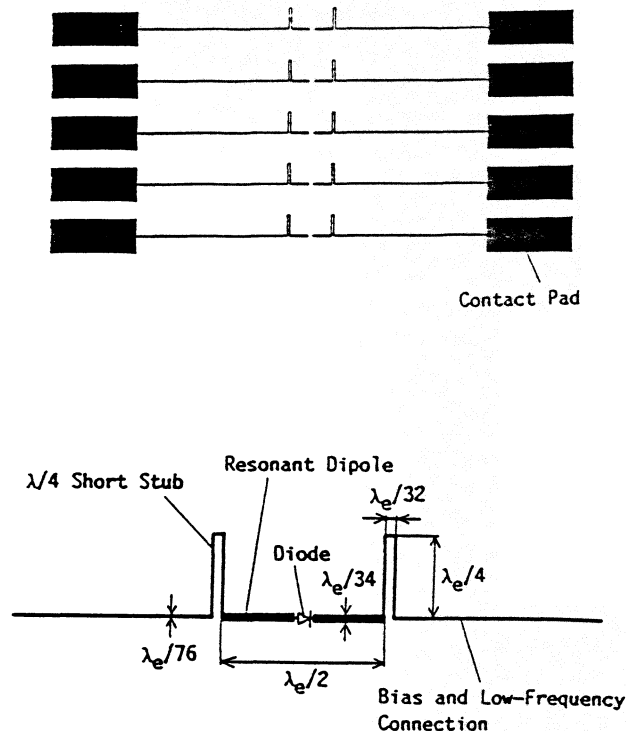


Fig. 6. The configuration of a trap-loaded dipole imaging array.

III. TRAP-LOADED ANTENNA IMAGIGN ARRAYS

The dipole configuration shown in Fig. 1 offers some difficulties to fabricate parallel array because of the obstruction of the bias and low-frequency leads. In order to avoid any complex circuit designs which may degrade radiation patterns or crosstalks, we have designed trap-loaded antenna configuration [5] shown in Fig. 6. In this structure, the leads are taken from the edges of the dipole through high impedance traps. Each trap consists of a quarter-wavelength long short-stub which offers high Q-value.

Fig. 7 shows measured radiation patterns for the trap-loaded dipole (a) and the Yagi-Uda configuration (b) with $2\ell_2$ of $0.418\lambda_d$ and d of $0.124\lambda_d$. Fig. 7 (a) also shows dipole patterns calculated by assuming sinusoidal standing waves which have large amplitude on the dipole, and small one on the $3\lambda_e$ long outer sections. Undesirable radiations from the waves on the outer sections degrade radiation patterns and cause larger sidelobes in the E-plane. The directivity of 3.7dB for the dipole and 5.9dB for the optimized Yagi-Uda have been measured at 50GHz experiment. The cross polarization level of the trap-loaded dipole have been measured less than 20dB down at $\phi=45^\circ$, which indicates the troublesome radiation from the traps can be neglected. The antenna input impedances become higher than those in the previous structure due to effects of the outer sections. The impedance of the dipole with $2\lambda_e$ long traps have been measured about 200Ω in the 5GHz model experiment. Hence these antennas may be useful for heterodyne detection because the RF impedance of the pumped diode is much larger than the small signal impedance. The total receptor 3dB bandwidth of 10% for the dipole and 8% for the Yagi-Uda have been measured at 50GHz band. The results show narrower bandwidths than the previous structure because of the additional of the high Q-value traps.

IV. MONOLITHIC PATCH ANTENNA IMAGING ARRAYS

Although the Yagi-Uda configurations have offered good performance and simple structure to fabricate, lack of efficient space is one of the disadvantage for constructing additional integrated circuits. This disturbs particularly fabricating two-dimensional array. Then we have proposed the lens-coupled patch antenna imaging array configuration which is very suitable for fabricating two-dimensional arrays using MMIC technique (Fig. 8).

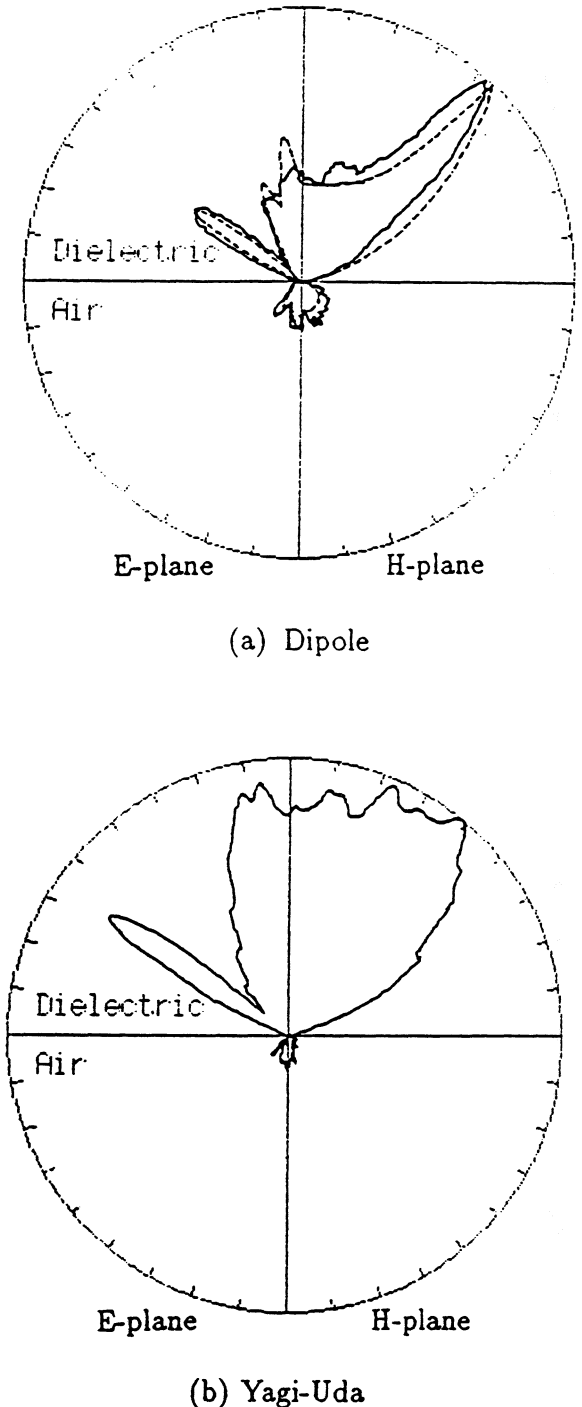


Fig. 7. The calculated and measured radiation patterns of a trap-loaded antenna on a dielectric hemisphere ($\epsilon_r=2.13$) of 100mm diameter. (a) Dipole, (b) Yagi-Uda ($2\ell_1=0.5\lambda_e$, $2\ell_2=0.418\lambda_d$, $d=0.124\lambda_d$). The scale is linear in power; —theory, - - -experiment at 50GHz.

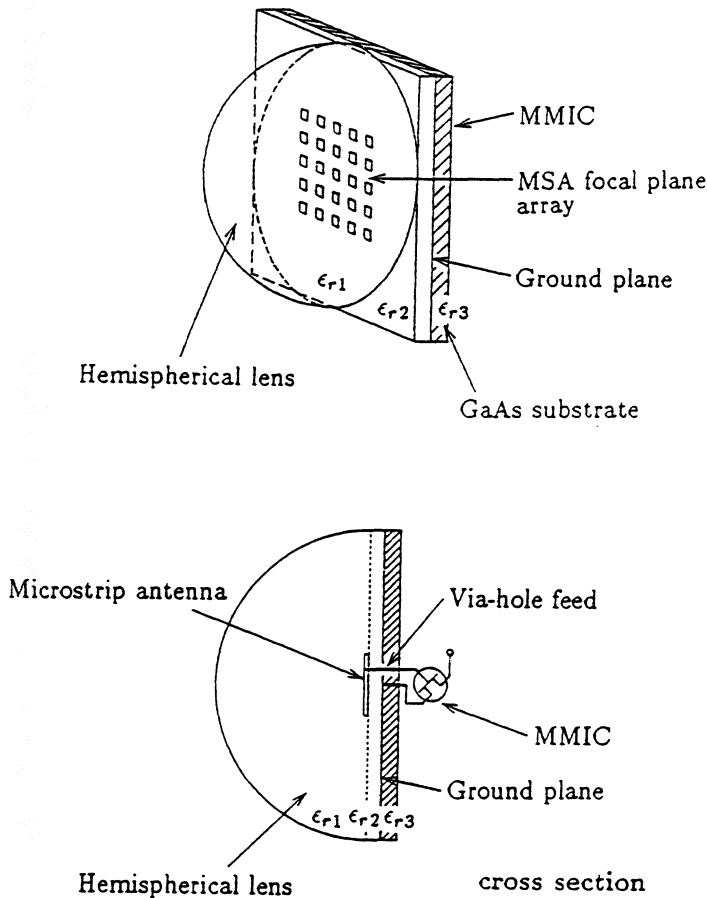


Fig. 8. The configuration of a two-dimensional microstrip patch antenna imaging array.

This array consists of two individual microstrip substrates separated by a common metal ground plane. The antennas are printed on the first substrate (ϵ_{r2}) covered with the low-loss dielectric lens (ϵ_{r1}). Each antenna is fed with a via-hole or coupling slot from the MMIC constructed on the second substrate (ϵ_{r3}). This second substrate offers the efficient space for fabricating additional integrated circuits: such as matching circuits, mixers, amplifiers, and leads. The antennas are ideally isolated from these circuits by the ground plane. Both the patch length a and patch width b are $0.5\lambda_d$, and the feed point (x_1, y_1) is $(0.25a, 0.5b)$.

Fig. 9 (a) shows calculated radiation patterns of the individual antenna versus ϵ_r which is defined by the ratio of the effective dielectric constant of the first substrate to the dielectric constant of the lens,

$$\epsilon_r \equiv \frac{\epsilon_{r2eff}}{\epsilon_{r1}} \quad (4)$$

If ϵ_{r1} equals ϵ_{r2} then the ratio ϵ_r becomes one, and then an ideal radiation pattern can be realized. This pattern is almost symmetrical and has neither any sidelobes nor troublesome radiations at the horizontal directions, which may offer low crosstalk and high beam coupling efficiencies to the incident beam. We have measured the radiation patterns at 50GHz band (Fig. 9 (b)). The results agree well with the theory: the calculated directivity is 9.8dB and the 3dB beam widths are 60° in the E-plane and 71° in the H-plane.

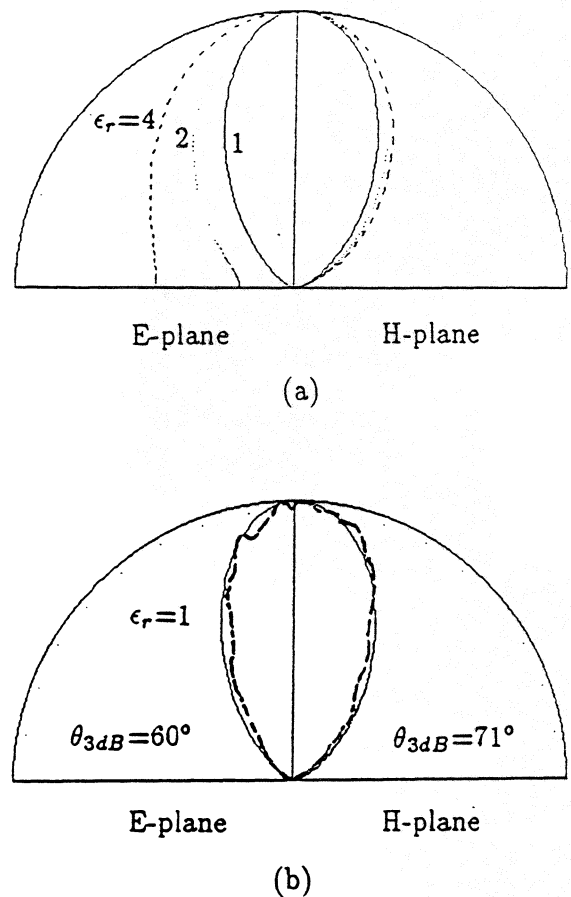


Fig. 9. The calculated and measured radiation patterns of a microstrip patch antenna on a dielectric hemisphere ($\epsilon_{r1}=2.13$) of 100mm diameter. (a) Theory for various ϵ_r , where ϵ_r is the ratio of the effective dielectric constant of the substrate (ϵ_{r2eff}) to the lens (ϵ_{r1}). (b) $\epsilon_r=1$; — theory, - - - experiment at 50GHz. The scale is linear in power.

The antenna input impedance of $85+j25\Omega$ has been calculated with a magnetic-wall model. The crosstalk

level of less than 20dB down in both E and H-plane when the element spacing is $0.7\lambda_d$ has been measured at the 6GHz model experiment. Fig. 10 shows the configuration of 3×3 element integrated patch array. The squares of dot-line show the patch antennas arrayed by the spacing of $0.7\lambda_d$. Matching circuits and low-pass filters are successfully constructed in each resolution unit. Since we can construct matching circuits in the second microstrip substrate, the mismatch loss between the antenna and a detector can be eliminated. Consequently this configuration is suitable for various kinds of detectors. The total 3dB bandwidth of 6% have been measured at 50GHz band experiment.

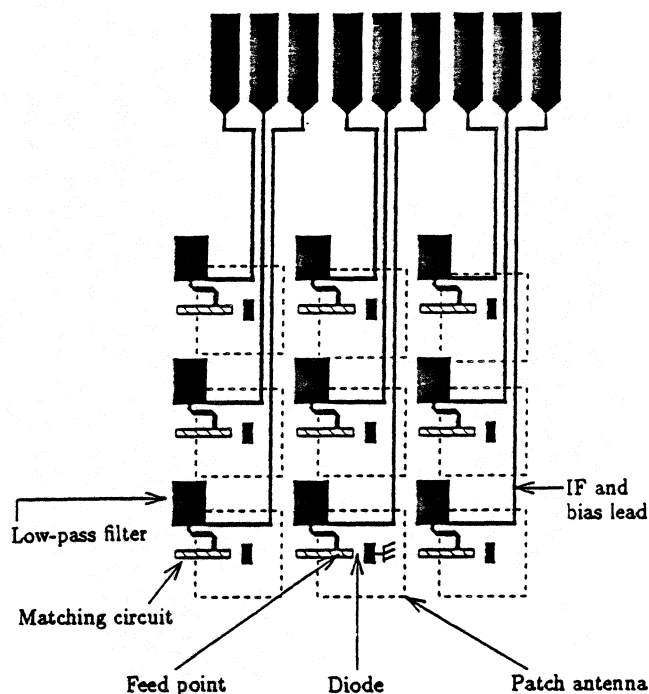


Fig. 10. The configuration of 3×3 monolithic microstrip patch antenna imaging array (bottom view).

V. APPLICATIONS

As a practical application, we have applied the 10 element trap-loaded parallel Yagi-Uda array to the Tsukuba GAMMA 10 plasma machine in order to measure the plasma density profile [5], for which we have constructed a 70GHz heterodyne phase imaging system. The IF frequency is 2MHz, the diode bias current is $400\mu\text{A}$, and the substrate lens is made of fused quartz ($\epsilon_r=4$) with a magnification of 4.0, and

other lenses are made with low-density polyethylene ($\epsilon_r=2.28$), giving a total magnification of 4.3. The system f -number of 1.0 determines the diffraction-limited sampling interval of 2.14mm ($1.0\lambda_d$) and cut-off frequency of 233m^{-1} , corresponding to a plasma dimension of 37mm. Fig. 11 shows the time evolutions of the line-density (a) and line-density profile (b) at the plug cell. The initial plasma produced by a plasma gun cannot be measured since the density is above the cut-off. The results are very close to those obtained by a millimeter-wave interferometer with scanning horn antennas, which is used for the cross-calibration.

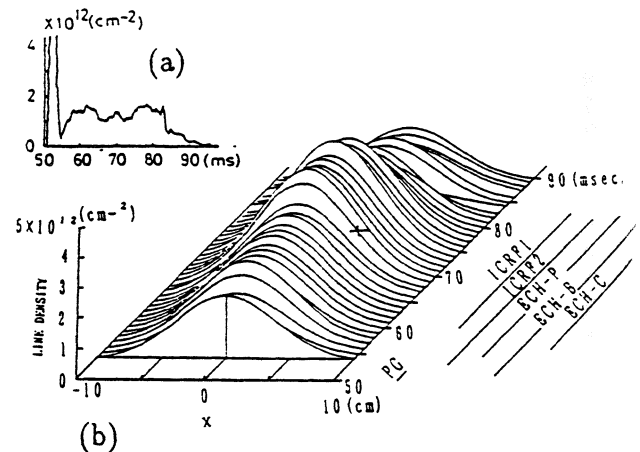


Fig. 11. The measurement of the time evolutions of the line-density (a) and line-density profile (b) at the plug cell in the Tsukuba GAMMA 10 plasma with a 10 element trap-loaded Yagi-Uda antenna imaging array at 70GHz. The time sequence is as follows: following the gun-produced plasma injection (PG), the plasma is heated with ion cyclotron range of frequency (ICRF) powers and electron cyclotron heating (ECH) powers.

VI. CONCLUSION

We have designed and investigated several kinds of lens-coupled antennas for operation at millimeter and submillimeter wavelength. The Yagi-Uda antennas have been successfully improved radiation patterns as well as impedance mismatch loss for small impedance detectors. Trap-loaded antennas have been designed in parallel arrays and successfully applied for plasma diagnostics. The lens-coupled patch antennas have been shown ideal radiation patterns and the stacked microstrip configuration has made possible to fabricate multi function arrays monolithically.

ACKNOWLEDGMENT

The authors wish to thank Prof. D. B. Rutledge and Dr. T. Suzuki for their valuable discussion and suggestions and also thank Sanyo Electric Co. Ltd. for kindly providing Schottky diodes. The authors also acknowledge Prof. A. Mase and Dr. K. Hattori of University of Tsukuba for collaborative research on the plasma diagnostics.

REFERENCES

- [1] K. Mizuno, Y. Daiku, and S. Ono, "Design of printed resonant antennas for monolithic-diode detectors," *IEEE Trans. Microwave Theory Tech.*, vol. MTT-25, pp. 470-472, Jun. 1977.
- [2] Y. Daiku, K. Mizuno, and S. Ono, "Dielectric plate antenna for monolithic Schottky-diode detectors," *Infrared Physics*, vol. 18, pp. 697-682, 1978.
- [3] K. Mizuno, K. Uehara, H. Nishimura, T. Yonekura, and T. Suzuki, "Yagi-Uda array for millimeter-wave imaging," *Electronics Letters*, vol. 27, No. 2, pp. 108-109, Jan. 1991.
- [4] D. B. Rutledge and M. S. Muha, "Imaging array," *IEEE Trans. Antennas Propagat.*, vol. AP-30, pp. 535-540, Jul. 1982.
- [5] K. Uehara, T. Yonekura, H. Nishimura, K. Miyashita, and K. Mizuno, "Millimeter-wave Yagi-Uda antenna imaging arrays," *The 3rd Asia-Pacific Microwave Conference Proceedings*, pp. 365-368, 1990.